ELSEVIER

Journal of Alloys and Compounds 231 (1995) 611–615

Journal of ALLOYS AND COMPOUNDS

A mathematical model for the cycle life of hydride electrodes

Y.Q. Lei, C.S. Wang, X.G. Yang, H.G. Pan, J. Wu, Q.D. Wang

Department of Materials Science and Engineering, Zhejiang University, Hangzhou 310027, People's Republic of China

Abstract

In this paper, a mathematical model for the cycling electrochemical capacity of hydride electrodes was deduced on the basis of activation and degradation of hydride materials. A cycle life model was deduced on introducing the activation and degradation factors into the electrochemical polarization equation which included concentration polarization, phase transformation polarization and electrochemical polarization. Experimental data on the TiNi hydride electrode were in good agreement with the deduced model. From this model, various factors affecting the cycle life were identified and the methods to enhance the cycle life were suggested.

Keywords: TiNi alloy; Hydride electrode; Cycle life; Discharge capacity

1. Introduction

In recent years many experimental investigation of the high rate discharge ability and cycle life of the hydride electrode have been reported [1,2]. So far no theoretical relation in one single equation has been deduced for the discharge capacity, discharge current and charge discharge cycle. Yayama [3] suggested that hydrogen diffusion in a hydride electrode was the rate-controlling step during both charge and discharge. On the basis of this assumption, Li et al. [4] deduced a relation between the discharge capacity and the discharge current density. Taking into account the ohmic losses between the electrolyte and in the metal hydride powder, the diffusion of hydrogen in metal and the charge transfer reaction at the surface of metal hydride particles, Viltanen [5] developed a mathematical model describing the discharge process of a metal hydride electrode, but cycle degradation was not considered in his model and it applied only to cylindrical electrodes.

It is generally accepted that many factors affect the activation and degradation process. Considering the oxidation of hydrogen absorption metallic elements as the main cause for capacity deterioration of hydride electrode, Willems [6], Wakao and Yonemura [7], Sawa et al. [8], Li et al. [9] and Züttel and coworkers [10] proposed their own cycle life equations. However, the values of the parameters in these equations were determined only from experimental capacity data; so it was only a semiempirical model.

In this paper, we first presented a mathematical model for the hydride electrode, i.e. the dependence of discharge capacity on discharge current and cycle life. Then the factors affecting the discharge capacity were analysed with a view to maximizing the discharge capacity.

2. Mathematical model

Here a mathematical model is set up for the discharge process of alloy grains. The hydrogen desorption process during discharge is considered to proceed in the following sequence: (a) nucleation and growth of the α phase from the β phase; (b) diffusion of hydrogen through the α phase to the surface of the particles; (c) electrochemical reaction $H_{ad} + OH^- = H_2O + e^-$. In general, all three steps affect the discharge process.

Let us assume that the hydride particles are spherical, the average radius of the hydride particles is r_0, the reaction occurs on the entire spherical surface simultaneously, the P_{eq} value of hydride is not far from 1 atm and discharge begins at the hydrogen concentration $C_{\beta\alpha}$, which is the hydrogen concentration of the alloy when fully charged uniformly throughout the whole β region and is the maximum

SSDI 0925-8388(95)01737-2

hydrogen concentration of the hydride at the equilibrium pressure P_{eq}, m is the number of spherical particles, $C_{\alpha\beta}$ is the maximum hydrogen concentration of the α phase at the α–β boundary, and C_α is the actual hydrogen concentration of the α phase at the boundary. C_α is less than $C_{\alpha\beta}$ because of the phase transformation barrier, and C_α and $C_{\alpha\beta}$ are much less than $C_{\beta\alpha}$, C_S is the surface concentration of the α phase. Fig. 1 illustrates the discharge process at quasi-steady state.

From the continuity of H flow in the α phase and Fick's first law,

$$4\pi mr^2 D_\alpha \frac{dC}{dr} = 4\pi mr_0^2 D_\alpha \left.\frac{dC}{dr}\right|_{r=r_0} = \frac{4\pi r_0^3 \rho m I}{3F} = \frac{4\pi r_0^3 \rho m I}{3F} \quad (1)$$

where I (mA g^{-1}) is the discharge current density per unit weight of electrodes ρ (g cm^3) is the density of the alloy.

Integrating Eq. (1) from $r = r_0$, $C = C_S$, $r = r_\alpha$, $C = C_\alpha$, we obtain

$$C_S = C_\alpha - \frac{Ir_0^2\rho}{3D_\alpha F}\left(\frac{r_0}{r_\alpha} - 1\right) \quad (2)$$

where r_α(cm) is the radius of the retained hydride particle.

When the electrode potential is 0.6 V, the surface concentration is close to zero, and the discharge capacity is equal to the value of F multiplied by the amount of hydrogen in the volume generated by the shaded area. Also the shaded area can be approximated to the square area (see Fig. 1).

The discharge capacity Q_d is given by

$$\begin{aligned} Q_d &\approx \tfrac{4}{3}\pi r_0^3 mF\left(C_{\beta\alpha} - \frac{C_\alpha}{2}\right)\left[1 - \left(\frac{r_\alpha}{0}\right)^3\right] \\ &\approx \tfrac{4}{3}\pi r_0^3 mF\left(C_{\beta\alpha} - \frac{C_{\alpha\beta}}{2}\right)\left[1 - \left(\frac{r_\alpha}{r_0}\right)^3\right] \\ &\approx Q_{max}\left[1 - \left(\frac{r_\alpha}{r_0}\right)^3\right] \end{aligned} \quad (3)$$

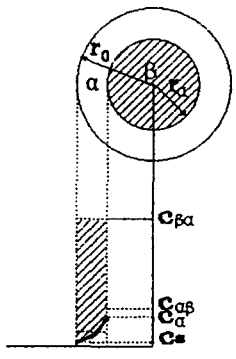

Fig. 1. Schematic diagram of hydrogen concentration in a spherical hydride particle.

where Q_{max}(mA h g^{-1}) is the maximum discharge capacity (close to the theoretical discharge capacity) because the interface between the α phase and the β phase is incoherent. The growth rate of the α phase is [11]

$$\frac{dr_a}{dt} = -K(C_{\alpha\beta} - C_\alpha) \quad (4)$$

where $1/K$(s cm^{-1} g^{-1}) constant of phase transformation barrier. In general, phase polarization is not very large, $C_\alpha \approx C_{\alpha\beta} \ll C_{\alpha\beta}$, i.e.

$$C_{\beta\alpha} - C_\alpha \approx C_{\beta\alpha} - C_{\alpha\beta} \quad (5)$$

r_α varies between 0 and 10^{-4} cm; r_α^2 can be approximated to

$$r_0^2 = \frac{r_0 r_\alpha}{2} \quad (6)$$

From the mass conservation on the boundary between the α and the β phases,

$$-(C_{\beta\alpha} - C_\alpha)\frac{dr_\alpha}{dt} = D_\alpha \left.\frac{dC}{dr}\right|_{r=r_\alpha} = \frac{Ir_0^3\rho}{3Fr_\alpha^2} \quad (7)$$

When electrochemical polarization and concentration polarization work simultaneously [12],

$$I = i_0 \frac{C_S}{C_{\alpha\beta}} \exp\left(\frac{\alpha F\eta}{RT}\right) \quad (8)$$

where i_0(mA g^{-1}) is the exchange current density and α(=0.5) is a symmetry factor. Combining Eqs. (2) and (5)–(8), Q_d can be written as

$$Q_d = Q_{max} \times \left[1 - \left(\frac{2D_\alpha/Kr_0(C_{\beta\alpha} - C_{\alpha\beta}) + 1}{(3FD_\alpha C_{\alpha\beta}/Ir_0^2)[1 - (I/i_0)\exp(-\alpha F\eta/RT)] + 1}\right)^3\right] \quad (9)$$

3. Experimental procedures

Alloys were prepared by melting the Ti (purity, 99.9%) and Ni (purity 99.9%) pellets in an arc furnace. Ingots were pulverized into fine powder by hydrogen decrepitation, through electrochemical charging and discharging cycling. The hydride electrodes were made by mixing the alloy powder with finely powdered electrolytic copper (300 mesh) at a weight ratio of 1:2. The mixture was cold pressed into small copper caps to form porous test electrodes of 10 mm diameter. The discharge capacity of each sample was determined by using the galvanostatic charging–discharging method in a trielectrode electrolytic cell. The counterelectrode and reference electrode were $Ni(OH)_2$ NiOOH and Hg/HgO in 6 M KOH respectively. The discharge cut-off potential was 0.6 V.

The exchange current density and polarization curve were tested by transient techniques [12].

4. Determination of parameters

4.1. Hydrogen concentration $C_{\alpha\beta}$ and $C_{\beta\alpha}$

$C_{\alpha\beta}$ and $C_{\beta\alpha}$ were determined on the discharge E–C–T curve for different cycle numbers.

4.2. Exchange current density i_0

For an oxide-covered metal electrode the exchange current density decreases strongly, approximately exponentially, with increasing oxide film thickness [13]. The thickness of TiO_2 usually increases parabolically (square root function) with increasing cycle number because of the corrosion protection action of TiO_2. In our experimental test, we found that i_0 decreased with decreasing potential (or decreasing hydrogen concentration) and increasing number of charge discharge cycles. Taking the average value at the $V=0.858$ potential as i_0, we can express the relation between the exchange current density and the cycle number in the following equation:

$$i_0 = 35\exp(-0.05N^{1/2}) \tag{10}$$

4.3. The relation of K and Q_{max} with the cycle number

The activation of a metal hydride electrode is affected by the following factors: (a) the increase in the surface area of alloy grains by pulverization and dissolution of some of the alloy component or their oxides [10] (by scanning electron microscopy (SEM), we found that the radius (r_0) of particles was 7.3×10^{-4} cm and the degree of pulverization was small because of the low volume expansion at the $\alpha\rightarrow\beta$ phase transformation for TiNi); (b) the decrease in activation energy barrier of phase transformation [14], as K increases with increasing number of charge–discharge cycles. Much evidence indicates that, during charge–discharge cycling, in the alloy, two-dimensional defects are developed in the alloy, which contribute to the observed increase in the rate of hydride formation. On the basis of the initial discharge capacity and that after cycling, the value of K in Eq. (9) is determined to be $6\times10^{-5}\exp(1.45N)$ cm g s^{-1}.

Degradation is believed to be caused by the following factors. Firstly there is the loss of the effective alloy weight by oxidation, the dissolution of these oxides and active components, the formation of stable hydride phase [15,16], and increase in contact electrical resistance caused by pulverization and oxidation of the surface of alloy particles. These effects cause C_{max} (or $C_{\beta\alpha}$) to decrease with increasing cycle number. The change in the degraded capacity is assumed to be proportional to the active capacity [10], i.e.

$$\frac{dQ_{max}}{dN} = \lambda Q_{max}$$

Because of the corrosion protection action of TiO_2, the above equation can be changed as follows:

$$\frac{dQ_{max}}{dN^{1/2}} = \lambda Q_{max}$$

and then

$$Q_{max} = A\exp(\lambda N^{1/2}).$$

The parameters A and λ were determined as 204 and -0.0216 respectively from E–C–T curves obtained at different cycle numbers. Secondly there is the decrease in the exchange current density, owing to surface oxidation. As TiO_2, is a semiconductor, i_0 of the TiNi electrode rapidly decreases with increasing cycle number, as expressed in Eq. (10).

4.4. Hydrogen diffusion coefficient D_α in TiNi alloy

$D_\alpha(=10^{-10}\exp(-0.002N^{1/2})$ was determined by the potentiostatic discharge method [1] at different cycle numbers.

4.5. Determining the kinetics equation of TiNi electrode (Table 1)

Table 1 gives the values of the parameters.

Substituting these values of parameters into Eq. (9), we obtain

$$Q_d = 204\exp(-0.0216N^{1/2}) \times\left[1-\left(\frac{0.63\exp(-1.45N+0.0196N^{1/2})+1}{(50.4/I)\exp(-0.002N^{1/2})-4.13\times10^{-3}\exp(0.048N^{1/2})+1}\right)^3\right] \tag{11}$$

5. Results and discussion

The cycle life and ability for high rate discharge tests were carried out for the $Ti_{50}Ni_{50}$ alloy. The curved surface calculated from Eq. (11) fits well with the test values (black spots) as shown in Fig. 2.

From the above analysis and experimental results we believe that factors affecting the degradation can be divided into two groups: one group contains thermodynamic parameters, such as C_α, and $C_{\alpha\beta}$; the other group contains the kinetic parameters D_α and i_0 and the geometric parameter r_0. The discharge capacity degradation is controlled by the thermodynamic degradation, i.e. Q_{max} is affected by intrinsic degra-

Table 1
The value of parameters

Parameter	Units	Value	Method
$C_{\alpha\beta}$	$H\,M^{-1}$	0.1	E–C–T curve
$C_{\beta\alpha}$	$H\,M^{-1}$	$0.86\exp(-0.0216N^{1/2})$	E–C–T curve
Q_{max}	$mA\,h\,g^{-1}$	$204\exp(-0.0216N^{1/2})$	E–C–T curve
i_0	$mA\,g^{-1}$	$35\exp(-0.05N^{1/2})$	Transient technique
D_α	$cm^2\,s^{-1}$	$10^{-10}\exp(-0.002N^{1/2})$	Transient technique
r_0	cm	7.3×10^{-4}	SEM
K	$cm\,g\,s^{-1}$	$6\times10^5\exp(1.45N)$	Discharge capacity
η	V	0.3	
F	mA h	26800	
	$kJ\,V^{-1}\,mol^{-1}$	96.39	
RT	$kJ\,mol^{-1}$	2.474	
α		0.5	

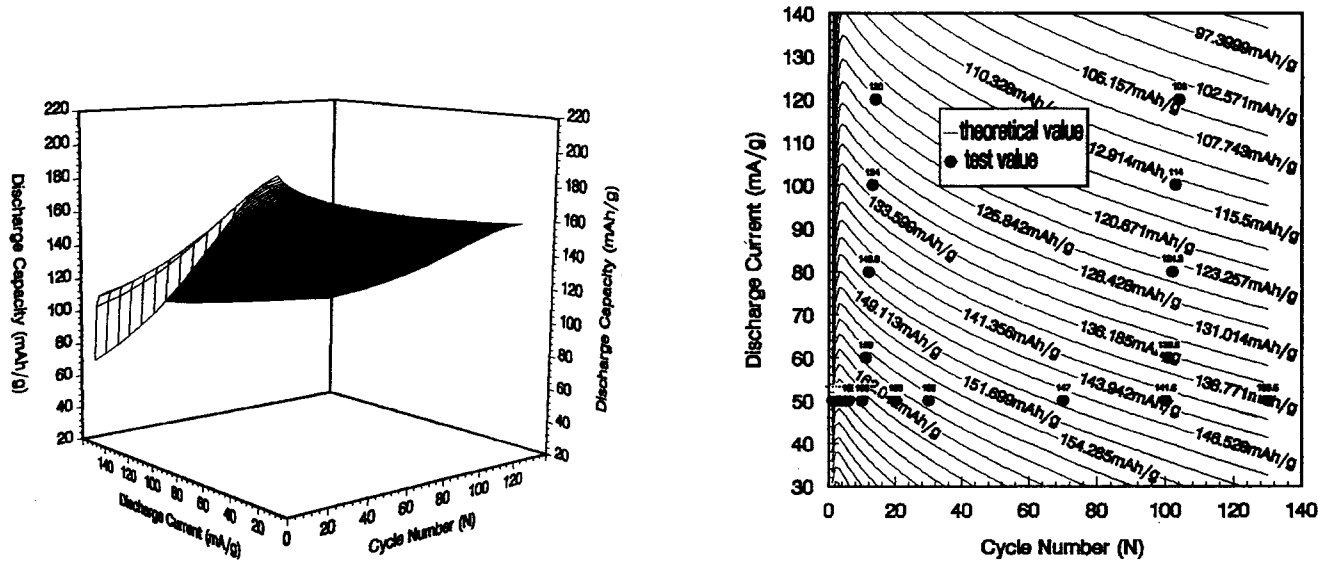

Fig. 2. Plot of the measured values of the capacity for TiNi samples (blank point) and model curve: (a) three-dimensional curved surface; (b) isodischarge capacity section.

dation [15] and corrosion degradation. For the electrode, generally, the corrosion degradation is more severe than the intrinsic degradation. The formation of insulating oxide layers caused not only a decrease in the alloy mass but also the loss of electrical grain-to-grain contact. In this case the electroless plating may enhance the cycle life noticeably. As for the kinetic factors, they can be divided into three groups: (a) phase transformation polarization K; (b) electrochemical polarization i_0; (c) concentration polarization D_α. Phase transformation polarization influences the process only in the first few cycles as the initial polarization coefficient is large (0.63) and cycling decline coefficient is also large (1.45). The phase transformation polarization increases with increasing discharge current density and the mechanical pressure applied at electrode formation. As the charge–discharge cycle continues, the concentration polarization gradually controls the polarization process, because the coefficient affecting the cycle is larger ($50.4I^{-1} > 4.13\times10^{-3}$) when the discharge current is not too large. However, because coefficient of the electrochemical polarization affecting the cycle is still larger than that of the concentration polarization ($0.048 > 0.002$), the polarization process eventually becomes controlled by chemical polarization. The curve for $I = 50\,mA\,g^{-1}$ also fits the test points well (Fig. 3(a)).

The ability of high rate discharge depends mainly on $D_\alpha, C_{\alpha\beta}, i_0$ and r_0. Increasing $C_{\alpha\beta}, D_\alpha$ and i_0 and decreasing r_0 first enhances the discharge kinetics of electrode. However, increasing $C_{\alpha\beta}$ and decreasing r_0 will lead to a decrease in Q_{max}, owing to a higher retained discharge capacity and faster oxidation. So extreme values for $C_{\alpha\beta}$ and r_0 exist. The curve calculated using Eq. (11) at $N = 10$ is compared with the test values in Fig. 3(b).

Eq. (9) was deduced from general electrochemical principles, without any limitations. It applies to all hydride electrodes including AB_2 and AB_5-type electrodes.

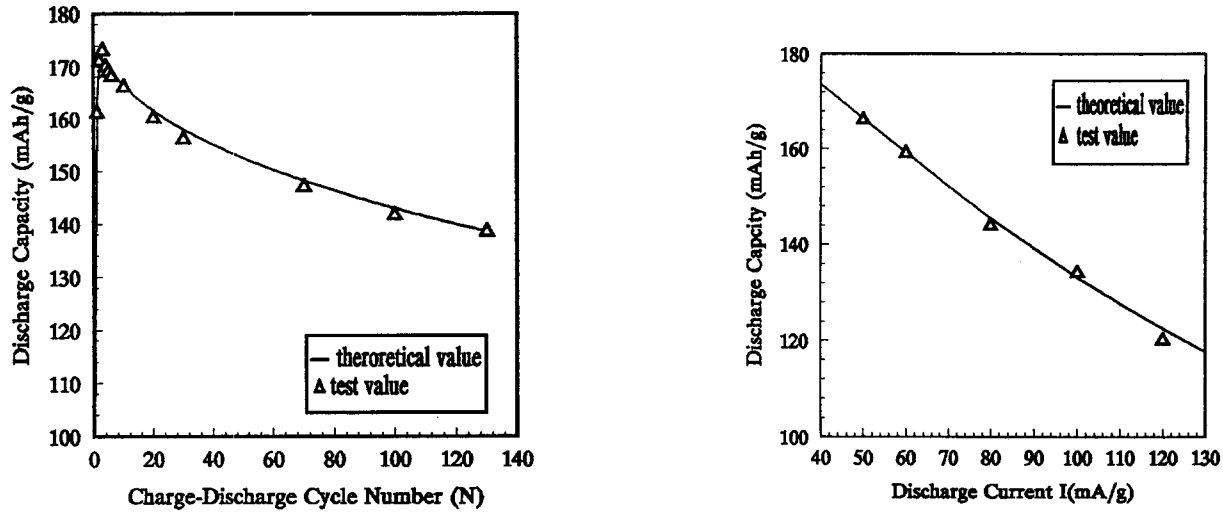

Fig. 3. Plot of model curve vs. measured sample value: (a) $I = 50\ mA\ g^{-1}$; (b) $N = 10$.

6. Conclusion

For alloy TiNi the activation is mainly controlled by phase polarization. Its degradation in charge–discharge cycling is determined by both thermodynamic degradation and kinetic degradation. The controlling step for polarization changes gradually from phase transformation to concentration polarization and finally to electrochemical polarization. The ability for high rate discharge also varies with charge–discharge cycling. At the first few cycles, it is dominated by the diffusion coefficient and later is controlled by the exchange current density.

Eq. (11) deduced from electrochemical principle fits the experimental data on TiNi-type hydride electrodes well. It is very useful for the high rate discharge capacity evaluation and the life test of hydride electrodes.

Acknowledgment

This project is supported by the National Natural Science Foundation of China.

References

[1] M.H.J. Van Rijswick, *Proc. Int. Symp. on Hydrides for Energy Storage, Geilo, 1977*, Pergamon, Oxford, 1978, p. 261.
[2] S. Wakao and Y. Yonemura, *J. Less-Common Met., 89* (1983) 481.
[3] H. Yayama, *Jpn. J. Appl. Phys., 23*(12) (1984) 1619.
[4] Z.P.Li, Y.Q. Lei, C.P. Chen, J. Wu and Q.D. Wang, *J. Less-Common Met., 172–174* (1991) 1260.
[5] M. Viltanen, *J. Electrochem. Soc., 140* (1993) 936.
[6] J.J.G. Willems, *Phillips J. Res., 39* (1984) 1.
[7] S. Wakao and Y. Yonemura, *J. Less-Common Met., 131* (1987) 311.
[8] H. Sawa, M. Ohta, H. Nakao and S. Wakao, *Z. Phys. Chem., NF, 164* (1989) 1527.
[9] Z.P. Li, Y.Q. Lei, B.H. Liu, J. Wu and Q.D. Wang, *Z. Phys. Chem., 183* (1994) 287.
[10] A. Züttel, F. Meli and L. Schlapbach, *J. Alloys Compd., 200* (1993) 157.
[11] D.A. Porter, *Phase Transformation in Metals and Alloy*, Van Nostrand Reinhold, New York, 1981, p. 300.
[12] Q.X. Cha, *Introduction to Kinetics of Electrode Processes*, Academic Press, Peking, 2nd edn., 1987, pp. 165–166 (in Chinese).
[13] J.OM. Bockris, B.E. Conway and R. White, *Modern Aspects of Electrochemistry*, No. 17, Plenum, New York, 1986, p. 391.
[14] E.H. Kisi, C.E. Buckley and E.M. Gray, *J. Alloys Compd., 185* (1992) 369.
[15] S.W. Lambert, D. Chandra and W.N. Chathey, *J. Alloys Compd., 187* (1992) 113.
[16] H.-H. Lee and J.Y. Lee, *J. Alloys Compd., 202* (1993) 23–28.